Chapter 14

Aerosol Direct Radiative Forcing: A Review

Chul Eddy Chung

Additional information is available at the end of the chapter

http://dx.doi.org/10.5772/50248

1. Introduction

Aerosols affect climate in multiple ways. Aerosol absorbs or scatters radiation in the atmosphere (so-called direct effect). Aerosols, except dust, interfere mainly with solar radiation. Some aerosols act as cloud condensation nuclei (CCN), thus affecting cloud albedo and lifetime (so-called indirect effect). Dark color aerosols can be deposited on sea ice, snow packs and glaciers, thus darkening the snow and ice surfaces, and enhancing the absorption of sunlight (so-called surface darkening effect). Some of the aerosols can absorb sunlight efficiently and heat the atmosphere. This heating can burn cloud (so-called semi-direct effect). Here, I offer an overview of the aerosol direct effect on solar radiation.

The effect of aerosols on climate is normally quantified in terms of aerosol radiative forcing. Aerosol radiative forcing is defined as the effect of anthropogenic aerosols on the radiative fluxes at the top of the atmosphere (TOA) and at the surface and on the absorption of radiation within the atmosphere. The effect of the total (anthropogenic + natural) aerosols is called aerosol radiative effect or total aerosol forcing. In this chapter, I discuss various parameters that affect aerosol direct radiative effect or aerosol direct radiative forcing.

τ	AOD	Aerosol Optical Depth
τ_a	AAOD	Absorption Aerosol Optical Depth; = (1−SSA)×AOD
α	AE	Ångström Exponent for Extinction
β	AAE	Absorption Ångström Exponent
	SSA	Single Scattering Albedo
	ASY	Asymmetry parameter

Table 1. Summary of acronyms and symbols.

Aerosol direct forcing can be, and has been, estimated purely from observations alone, but the estimation has been done predominantly by a radiation model. A variety of radiation

models have been used for estimating aerosol direct forcing and all of them have common input variables such as AOD (or extinction coefficient), SSA (Single Scattering Albedo), ASY (Asymmetry Parameter). These input variables have been obtained by aerosol simulation models or by aerosol observations. I review the input variables and also give an estimate of aerosol direct radiative effect.

2. Aerosol optical properties

2.1. Aerosol Optical Depth (AOD)

When a beam of light is attenuated, we call this attenuation *extinction*. Extinction is a result of scattering plus absorption. Aerosols can scatter and absorb light, and the attenuation due to aerosol is called aerosol extinction. Aerosol extinction will weaken the light intensity from I_λ to $I_\lambda + dI_\lambda$ after traversing a thickness ds in the direction of its propagation. λ represents wavelength. Then, the following equation holds:

$$d\, I_\lambda = -k_\lambda \varrho I_\lambda\, ds \tag{1}$$

where ρ is the density of the material, and k_λ denotes the mass extinction cross section (in units of area per mass). $k_\lambda \rho$ is referred to as the *aerosol extinction coefficient*, whose units are given in terms of length (typically, cm^{-1}). The aerosol extinction coefficient is the sum of the aerosol scattering coefficient and the aerosol absorption coefficient. Over the globe, the aerosol extinction coefficient is a function of space (X-Y-Z), time (T) and wavelength. The aerosol optical depth τ is a vertical integral of the aerosol extinction coefficient from the earth surface (Sfc) to the top of the atmosphere (TOA), as follows:

$$\tau_\lambda = \int_{Sfc}^{TOA} k_\lambda \rho dz \tag{2}$$

AOD is not a function of height. AOD is the sum of AAOD (Absorption Aerosol Optical Depth) and SAOD (Scattering Aerosol Optical Depth). AAOD (τ_a) is the vertical integral of the aerosol absorption coefficient.

Another way to understand AOD is that it describes column-integrated aerosol amount in an optical sense. When aerosol mass amount is doubled, AOD should also be doubled. Aerosol mass amount, however, is not directly related to aerosol forcing, as AOD is. Furthermore, satellite observations can be used to infer AOD, not aerosol mass amount. For these collective reasons, AOD is the most fundamental variable for aerosol-climate interaction. AOD is also called AOT (Aerosol Optical Thickness). Combining Eq. 1 and Eq. 2, we find that $I_\lambda(\text{Sfc}) = I_\lambda(\text{TOA}) \times \exp(-\text{AOD})$. Thus, aerosols with AOD of 1.0 reduce the light beam (i.e., direct radiation) by e^{-1}. e^{-1} is 0.368. In this case, the sun will appear largely hidden by aerosols at the surface. AOD of 1.0 represents a very dense aerosol layer.

AOD is a function of wavelength. The community generally uses the 550 nm value for the standard AOD. Fig. 1 shows how aerosol forcing changes with respect to AOD. When AOD is small (say, < 0.3), doubling AOD leads to doubled forcing. When AOD becomes large, added AOD translates into a smaller increase in forcing.

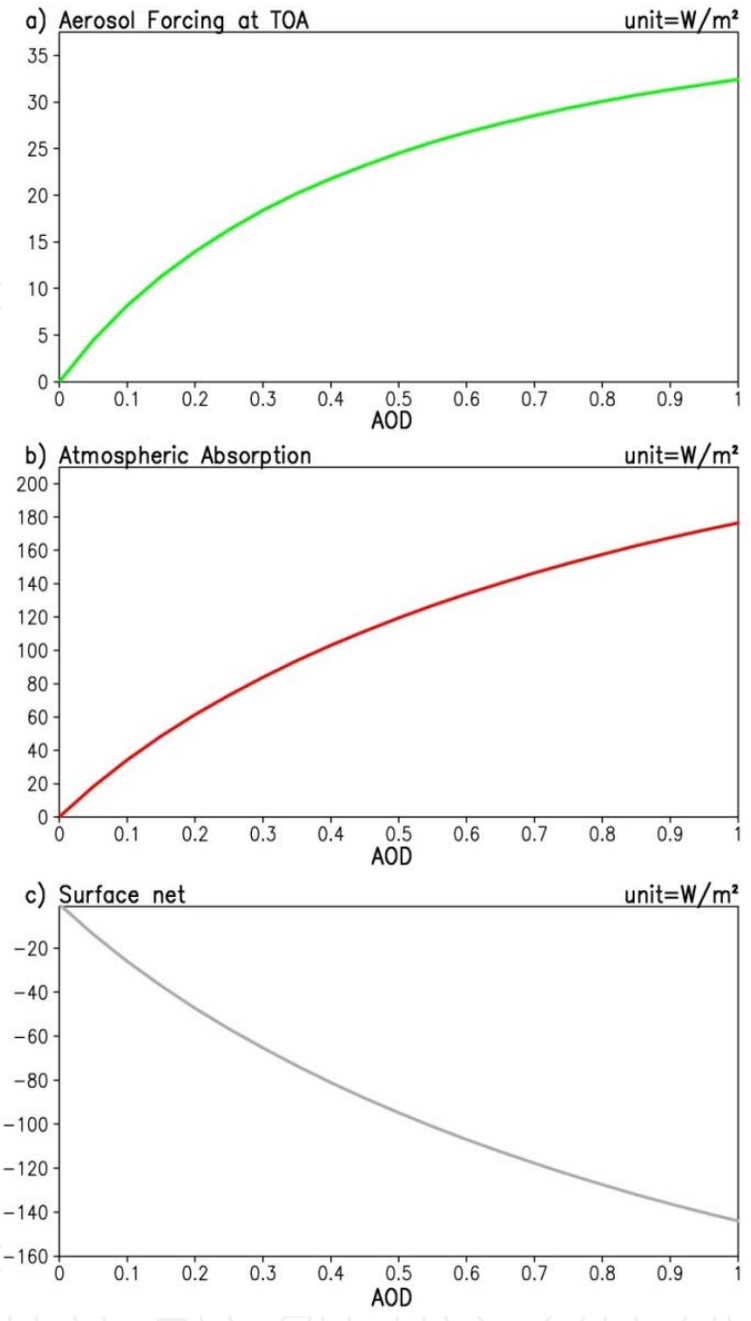

Figure 1. Annual-mean clear-sky aerosol forcing as a function of AOD at 550 nm. The simulation is made with a Monte-Carlo radiation model as in Chung et al. (2005), which only considered solar radiation. Specified parameters are SSA=0.19 at all the wavelengths, ASY=0.7 at 550 nm, α=1.4, and land surface albedo of 0.15 at a latitude of 21°N.

2.2. Single Scattering Albedo (SSA)

When photons hit an aerosol particle, some photons will be scattered while the other will be absorbed. The SSA is defined as the ratio of the scattering to the extinction. Extinction is the sum of scattering and absorption. When photons are scattered, the wavelength remains unchanged. SSA is a function of wavelength.

SSA can be computed in case of a single particle, aerosol layer or column integrated aerosols. For a single particle, the number of scattered/absorbed photons can be counted to calculate the SSA, or the scattering/extinction cross section can be measured/calculated. For a single particle, its SSA depends on particle size, particle shape and material refractive index. For an aerosol layer, the aerosol extinction/scattering coefficient can be used to compute the SSA. For column-integrated aerosols, AOD and SAOD can be used to compute the column-integrated SSA. For a group of aerosols, aerosol size distribution will affect the SSA.

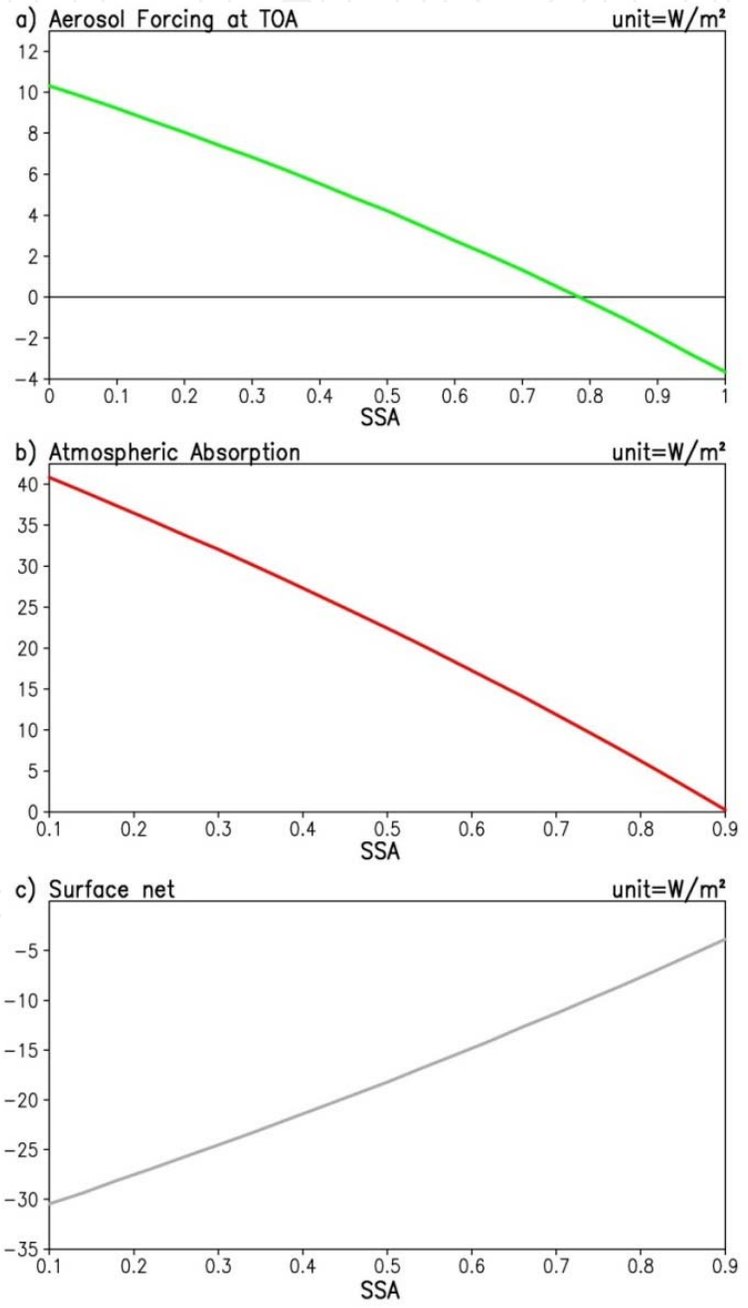

Figure 2. Annual-mean clear-sky aerosol forcing as a function of SSA. SSA is prescribed to be wavelength independent here. AOD at 550 nm is 0.1, and the rest parameters are as in Fig. 1.

Fig. 2 shows how aerosol forcing changes with respect to SSA. It is very important to note that the forcing at the TOA depends crucially on SSA. When SSA is low, the TOA forcing is positive. Conversely, the TOA forcing becomes negative with high SSAs. Aerosol forcing typically refers to the TOA forcing. Another important feature is that the surface forcing becomes larger (more negative) with lower SSA given a fixed AOD. In other words, absorbing aerosols are more effective surface dimmers.

SSA is one of the aerosol intrinsic properties. Aerosols can be classified in terms of aerosol species, the most common of which are BC (black carbon), OM (organic matter), dust, sulfate, sea salt and nitrate. Sea salt, sulfate and nitrate are known to have close to 1.0 in SSA. OM was in the past treated as 100% scattering (Myhre et al., 2007; Stier et al., 2007), but is now widely accepted to have significant absorption due to brown carbon (Andreae & Gelencsér, 2006) (BrC) component. It appears that there are large differences in the estimated magnitude of BrC absorption (Alexander et al., 2008; Chakrabarty et al., 2010; Hoffer et al., 2006). Magi (2009, 2011) analyzed air-craft data over the southern Africa and concluded that OM SSA is 0.85±0.05 at 550 nm. There is a possibility that OM SSA over the southern Africa might differ from that over other regions.

Magi (2009, 2011) also gives BC SSA. According to his field study, BC SSA is 0.19±0.05 at 550 nm. BC SSA of 0.19 is very close to 0.185 from a theoretical calculation of BC aggregates by Chung et al. (2011) and also close to 0.18 from a laboratory study by Schnaiter et al. (2005). Many studies use a very high BC SSA (typically near 0.3), and this high BC SSA results from an assumption that BC is a spherical particle. BC has a cluster structure consisting of many monomers, and Chung et al. (2011) considered the cluster structure to derive the BC SSA. When BC is assumed to be spherical, Chung et al. (2011) found BC SSA to be 0.32.

Dust SSA has been estimated to be about 0.9 by Müller et al. (2010) and 0.92 by Eck et al. (2010) at 550 nm. When dust is transported over polluted areas, non-dust particles such as BC are often attached to dust. These two field studies (Müller et al., 2010; Eck et al., 2010) probably reported polluted dust SSA. Pure dust SSA is likely to be greater than 0.92. The combination of different aerosols will determine the aerosol SSA. When aerosols are BC rich, e.g., the SSA will be low thanks to the BC component. Thus, aerosol SSA is indicative of the relative abundance of each aerosol species.

2.3. Asymmetry Parameter (ASY)

When aerosols scatter light, the phase function describes the angular distribution of scattered energy. The phase function P(cosΘ) is a normalized function, such that

$$\int_0^{2\pi}\int_0^{\pi}\frac{P(\cos\Theta)}{4\pi}\sin\Theta\, d\Theta\, d\phi = 1 \quad (3)$$

where Θ refers to the angle between the direction of incoming light and that of the scattered light. When $\Theta < \pi/2$, the scattering is called forward scattering, while the scattering is backward when $\Theta > \pi/2$.

The asymmetry parameter, or asymmetry factor, g is defined as follows:

$$g = \frac{1}{2}\int_{-1}^{1} P(\cos\Theta)\cos\Theta \, d\cos\Theta \quad (4)$$

When the forward scattering is as much as the backward scattering, ASY becomes zero. ASY increases as the forward scattering dominates over the backward scattering. Larges particles have higher ASY. In the atmosphere, monthly-mean aerosol ASY ranges from 0.6 to 0.82 (from AERONET data analysis). AERONET (Holben et al., 2001) is a ground-based network of sun photometers located at over hundreds of stations around the world.

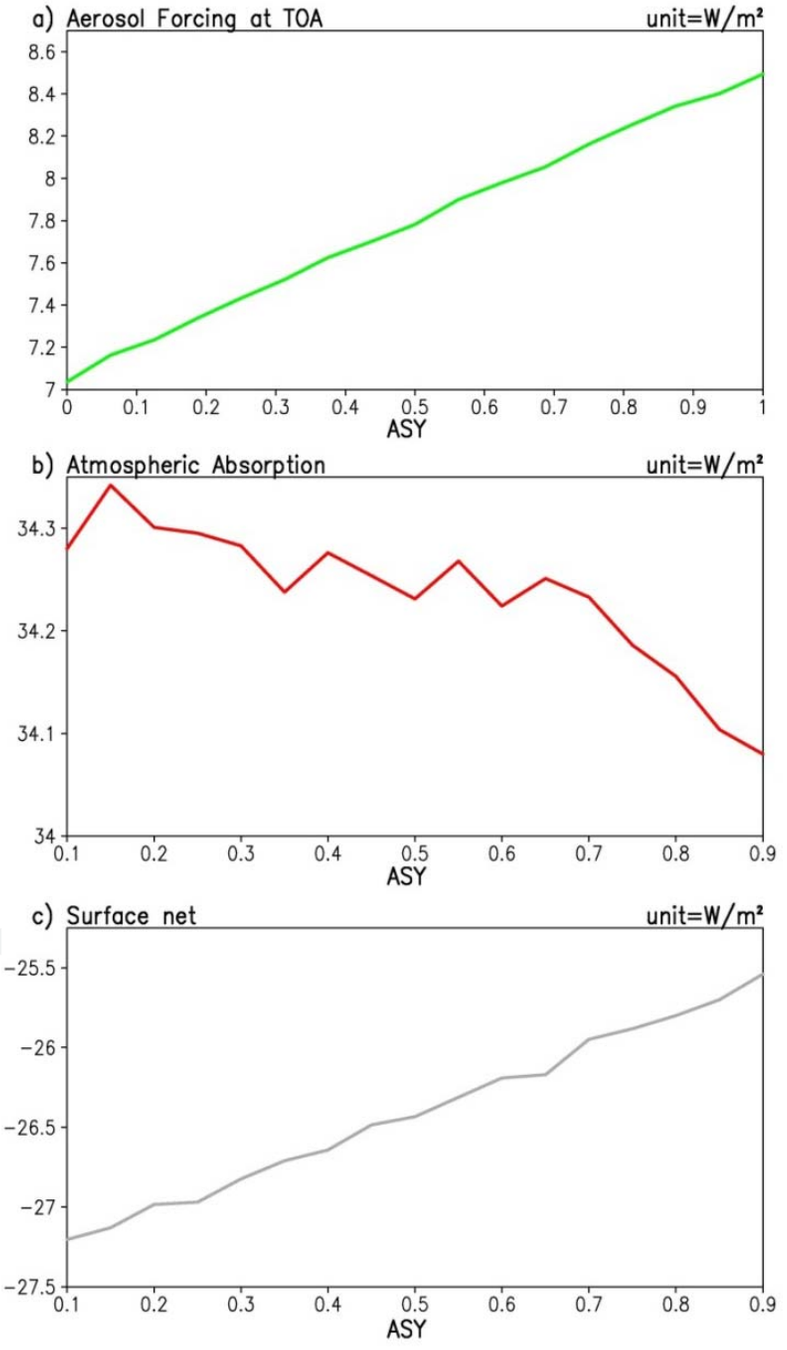

Figure 3. Annual-mean clear-sky aerosol forcing as a function of 550 nm ASY. AOD is 0.1, and the rest parameters are as in Fig. 1.

ASY has large impacts on aerosol forcing at the TOA but have little impacts on the atmospheric aerosol forcing (Fig. 3). This is because ASY does not change aerosol absorption which dominates the atmospheric forcing. Large ASYs are associated with large aerosol forcing at the TOA because aerosols with large ASY less scatter the solar radiation back to the space.

2.4. Ångström exponent (α)

α describes the wavelength dependence of AOD (or the aerosol extinction coefficient). In case of AOD Ångström exponent, the definition is as follows:

$$\mathrm{AOD}(\lambda) = \mathrm{AOD}(\lambda_R)\left(\frac{\lambda}{\lambda_R}\right)^{-\alpha} \quad (5)$$

λ_R is the reference wavelength, and is typically 550 nm. α cannot be negative, and can be as high as 4.0. Lower α means that aerosol extinction is more independent of wavelength, which is the case for larger particles. Large particles are associated with lower α and higher ASY.

Fig. 4 shows the effect of increasing α on aerosol forcing. As α increases, the total aerosol extinction of broad-band solar radiation decreases. Thus, large α is associated with slightly less aerosol forcing.

3. Other factors controlling aerosol forcing

In Section 2, I gave an overview of aerosol optical properties and explained how these properties affect aerosol forcing. Aerosol forcing is also influenced by non-aerosol properties, notably the surface albedo and low-level cloudiness.

The surface plays an important role in case of absorbing aerosols (i.e., aerosols with low SSA). As Fig. 5 shows, higher albedo (i.e., more reflection at the surface) increases aerosol absorption and thus aerosol forcing at the TOA as well as in the atmosphere. Higher albedo increases aerosol absorption because absorbing aerosols absorb not just the downward solar radiation but also the reflected upward radiation. Higher albedo also decreases aerosol scattering back to the space, further contributing to higher aerosol forcing at TOA. Ice, snow and desert have high surface albedo.

Low-level cloud reflects solar radiation effectively, and so absorbing aerosols above low cloud have more absorption, as demonstrated by Podgorny and Ramanathan (2001). Thus, absorbing aerosols above low cloud enhance aerosol forcing, just like absorbing aerosols over reflective surfaces. The difference between low cloud and highly-reflective surface is that aerosols can be located below or above low cloud. Zarzycki and Bond (2010) studied absorbing aerosol forcing with respect to low cloud. They found that BC aerosols above low clouds explain about 20% of the global burden but 50% of the forcing.

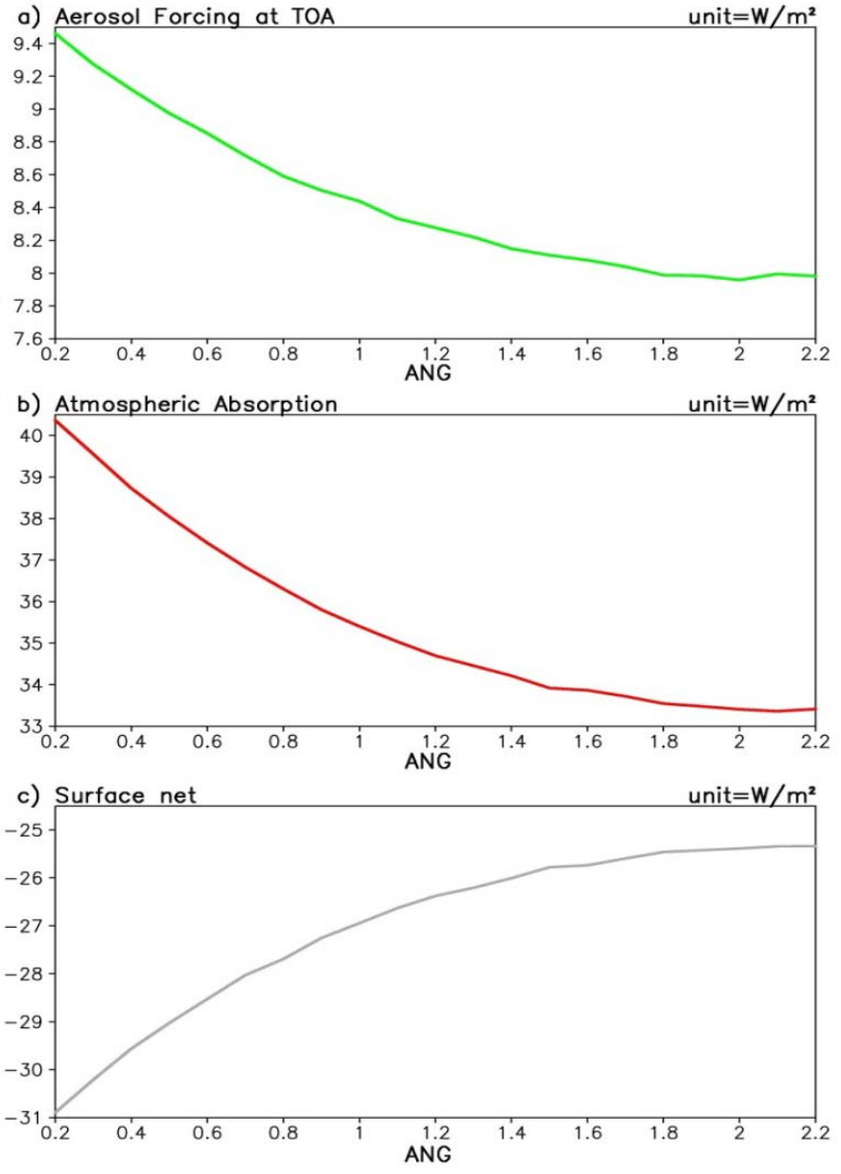

Figure 4. Annual-mean clear-sky aerosol forcing as a function of α. AOD at 550 nm is 0.1, and the rest parameters are as in Fig. 1.

4. Global distribution of aerosol optical properties

Here, I present observationally-constrained estimates of aerosol optical properties over the globe. The principal observation used here is AERONET (Aerosol Robotic NETwork), which is a ground-based network of measuring aerosol optical properties (Holben et al., 2001) as mentioned earlier. There are hundreds of AERONET sites worldwide, and all the sites are located over the land or an island. I use the monthly Level 2.0 from Version 2 product for the period 2001–2009. In this dataset, values are pre- and post-field calibrated, cloud screened and quality assured. AERONET offers AOD, SSA and ASY at multiple wavelengths. Where necessary, I logarithmically interpolated AOD and linearly interpolated SSA/ASY to the desired wavelength.

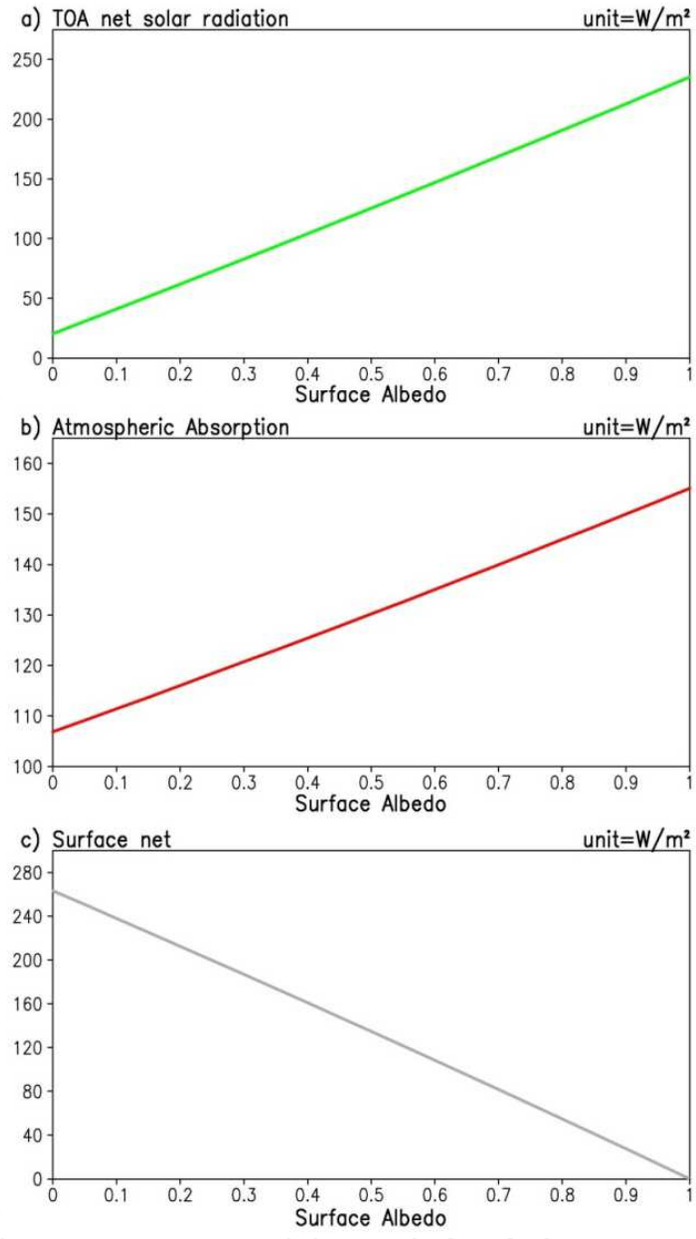

Figure 5. Figure 5. Annual-mean clear-sky aerosol forcing as a function of land surface albedo. AOD is 0.1, and the rest parameters are as in Fig. 1.

4.1. AOD at 550 nm

AERONET offers world-wide but sparsely-located AODs. To get globally gridded AOD, I use satellite observations from MODIS (MODerate resolution Imaging Spectro-radiometer) and MISR (Multi-angle Imaging Spectro-Radiometer). MODIS is a satellite sensor on board Terra satellite and Aqua satellite. I downloaded Collection 5.1 Aqua and Collection 5.0 Terra M3 AODs at 550 nm. Terra AOD and Aqua AOD on the 1º×1º resolution were converted to monthly combined AOD on the T42 resolution using following algorithm: If there are at least 5 values from either satellite in each T42 gridbox, a median is calculated in order to remove outliers. Then, 2001–2009 climatology for each calendar month is computed. As for

MISR AOD, I downloaded the CGAS MIL3MAE.4 product. Processing MISR AOD is similar to that of MODIS AOD.

I put together AERONET, MODIS and MISR AODs at 550 nm in the following. 1) I fill the gaps in MODIS AOD with MISR AOD using the iterative difference-successive correction method developed by Cressman (1959). MODIS does not give AOD over desert areas where MISR offers AOD. 2) The remaining gaps in MODIS+MISR AOD are filled with GOCART AOD again using Cressman(1959)'s method. 3) The spatial pattern in MODIS+MISR+GOCART AOD is coupled with the sparsely-distributed AERONET AOD values, using Chung et al. (2005)'s technique, as below.

$$N\_AODj = MMG\_AODj \times \frac{\sum_i \frac{AERONETj,i}{dj,i^4}}{\sum_i \frac{MMG\_AODj,i}{dj,i^4}} \tag{6}$$

Where N_AODj is the adjusted new value of the AOD at grid j, *AERONETj,i* is an AERONET_ AOD at station location i nearby the grid j, dj,i is the distance between j and i, and *MMG_AODj,i* is the MODIS+MISR+GOCART_AOD at the grid of *AERONETj,i*. Eq. 6 is applied for each calendar month. In this assimilation method, the order of influence is AERONET > MODIS > MISR > GOCART.

Fig. 6 visualizes the assimilated AOD. AOD is large over deserts such as the Sahara and the Gobi and their downstream areas. AOD is also large over biomass burning and fossil fuel combustion areas such as East Asia, South Asia, southern Africa and Amazon.

4.2. SSA at 550 nm

To get global SSA, I put together AERONET data and GOCART simulation as follows. First, GOCART SSA is computed using GOCART AODs as follows:

$$\mathrm{SSA}(\lambda_R) = (0.741 \times \tau_{CA}(\lambda_R) + 0.957 \times \tau_D(\lambda_R) + \tau_{rest}(\lambda_R))/\tau(\lambda_R). \tag{7}$$

CA represents carbonaceous aerosols. D represents dust. 0.957 is dust SSA. This number comes from AERONET SSA over the sites that give AAE around 2.41 ~2.42. CA SSA of 0.741 is chosen to minimize the global/annual mean difference between GOCART SSA and AERONET SSA.

Then, these GOCART SSAs are further adjusted by AERONET SSA as below.

$$\left(1 - \mathrm{N\_SSAj}\right) = \left(1 - G\_SSAj\right) \times \frac{\sum_i \frac{1 - AERONETj,i}{dj,i^4}}{\sum_i \frac{1 - G\_SSAj,i}{dj,i^4}} \tag{8}$$

Like Eq. 6, Eq. 8 maximizes the influence of AERONET data. By applying Eq. 8, the final SSA has observational constraint on regional scales.

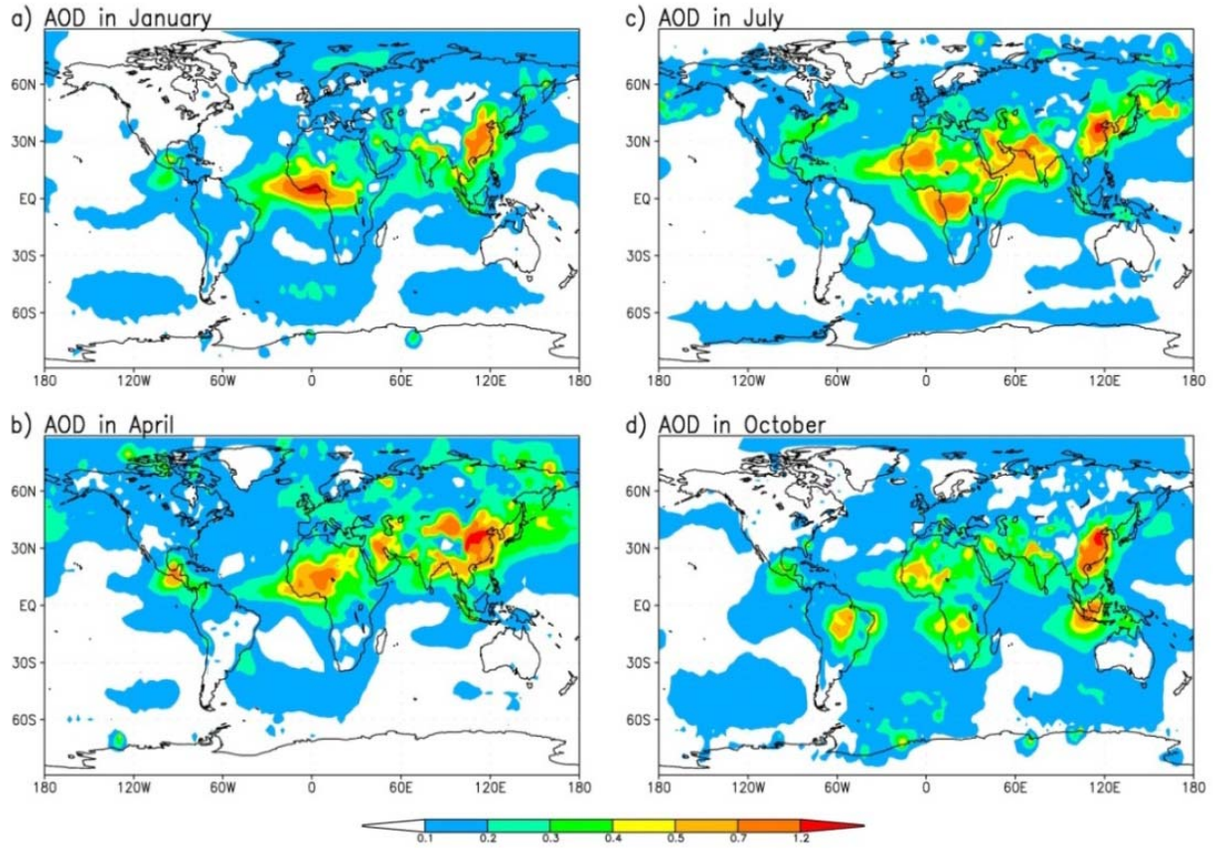

Figure 6. 2001–2009 Aerosol Optical Depth (AOD) at 550 nm, as derived by AERONET, MODIS and MISR observations.

Fig. 7 shows global aerosol SSA at 550 nm. Low SSA means absorbing aerosols. Typically, aerosols with SSA < 0.9 are considered absorbing. As the figure shows, heavy biomass burning areas such as the southern Africa show lowest SSA. This is because these areas emit large amounts of BC and relatively smaller amounts of scattering aerosols such as sulfate. Over much of the ocean, dominant aerosols are sea salt which has close to 1.0 in SSA.

4.3. ASY at 550 nm

To get global ASY, I put together AERONET data and GOCART simulation as follows. First, GOCART ASY is computed using GOCART SAODs as follows.

$$\mathrm{ASY}(\lambda_R) = (0.62 \times \mathrm{SAOD}_{CA}(\lambda_R) + 0.69 \times \mathrm{SAOD}_{sul}(\lambda_R) + 0.66 \times \mathrm{SAOD}_{D}(\lambda_R) \quad (9)$$
$$+0.778 \times \mathrm{SAOD}_{fs}(\lambda_R) + 0.85 \times \mathrm{SAOD}_{cs}(\lambda_R))/\mathrm{SAOD}(\lambda_R).$$

$\mathrm{SAOD}_{sul}(\lambda_R)$ refers to SAOD at 550 nm for sulfate. "fs" refers to fine sea salt, and "cs" refers to coarse sea salt. The numbers 0.62, 0.69 and 0.66 are chosen to match AERONET ASY. The numbers 0.778 and 0.85 came from the OPAC (Optical Properties of Aerosols and Clouds) data (Hess et al., 1998). GOCART SAOD is computed from AOD and SSA, where SSA is assigned in the following: 0.19 for BC, 0.85 for OM, 0.96 for dust and 1.0 for the rest. See section 2.2 for these numbers.

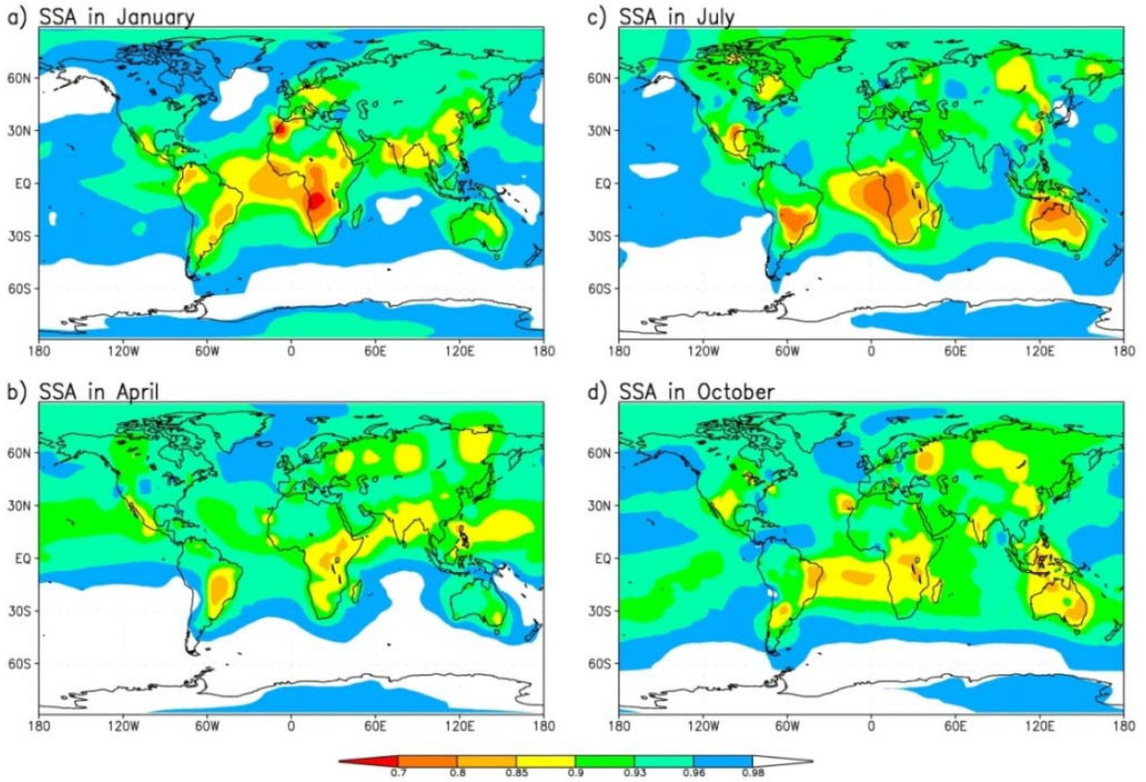

Figure 7. 2001–2009 Single Scattering Albedo (SSA) at 550 nm, as derived by AERONET and GOCART simulation.

Finally, these GOCART ASYs are adjusted by AERONET ASYs as below.

$$\mathrm{N\_ASYj} = \mathrm{G\_ASYj} + \frac{\sum_i \frac{AERONETi,j - G\_ASYj,i}{dj,i^4}}{\sum_i \frac{1}{dj,i^4}} \tag{10}$$

By applying Eq. 10, the final ASY has observational constraint on regional scales. Fig. 8 shows global ASY at 550 nm. Again, low ASY is associated with small particles. As demonstrated in Fig. 8, biomass burning areas tend to show low ASY. This is because biomass burning aerosols consist mainly of BC and OM and these two aerosol species are the smallest species. Since BC merely scatters, biomass burning aerosol ASY largely represents OM ASY. Fossil fuel combustion areas also show relatively low ASY. Large ASY values are seen over deserts and their downstream areas as well as over the ocean, because dust and sea salt are the biggest aerosols.

5. Global aerosol forcing

In section 4, I presented observationally-constrained AOD, SSA and ASY at 550 nm. In a method similar to the ASY assimilation, I generate observationally-constrained α and co-albedo Ångström exponent. Co-albedo is 1–SSA. Now, I have all the aerosol input

parameters needed to compute aerosol forcing except its vertical profile. The vertical profile and the radiation model are as in Chung et al. (2005), where the Monte-Carlo Aerosol Cloud Radiation (MACR) model was adopted with the observed cloud effects from the ISCCP (International Satellite Cloud Climatology Project). All the calculations are for solar radiation and for direct effects.

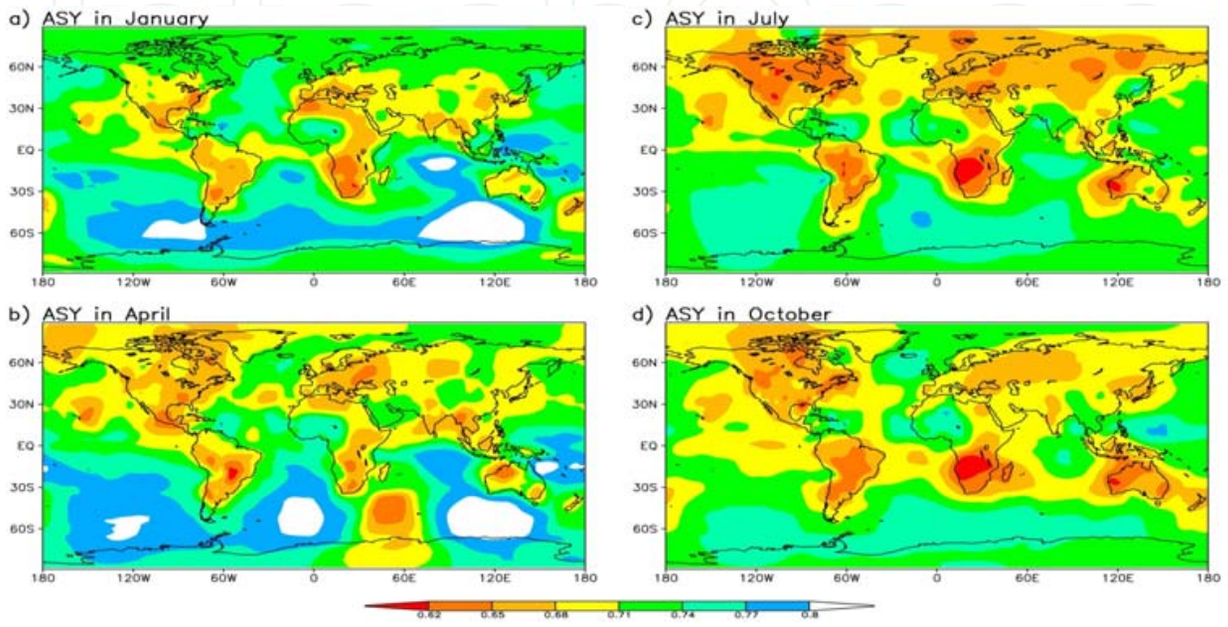

Figure 8. 2001–2009 asymmetry parameter (ASY) at 550 nm, as derived by AERONET and GOCART simulation.

Fig. 9 shows the total (natural + anthropogenic) aerosol forcing over the globe. The forcing is mostly negative, and large negative values tend to be associated with high AOD, i.e., large aerosol burden in the atmosphere. Some areas have significantly positive forcing instead. For example, the aerosols over the eastern tropical Atlantic (between Eq. and 20ºS) have huge positive forcing. This positive forcing is aided by low level cloud. To be sure, we repeated the radiation calculation without cloud (Fig. 10). The clear-sky forcing eliminates this positive-forcing feature. The remaining positive forcing in Fig. 10 is all over highly reflective surfaces such as deserts, ice. In the absence of high sulfate albedo and low cloud, the aerosol forcing is negative everywhere.

Near-zero forcing in Fig. 9 is usually associated with very little aerosol. However, the near-zero forcing that occurs between significantly positive and significantly negative forcings has a sizable amount of aerosols. Although these aerosols have near-zero forcing at the TOA, they always have large positive forcing in the atmosphere or large negative forcing at the surface. The cancellation between the surface forcing and the atmosphere forcing occurs makes the zero forcing at the TOA. This cancellation occurs when the aerosol SSA is within a certain range associated with certain surface albedo and the presence of low clouds.

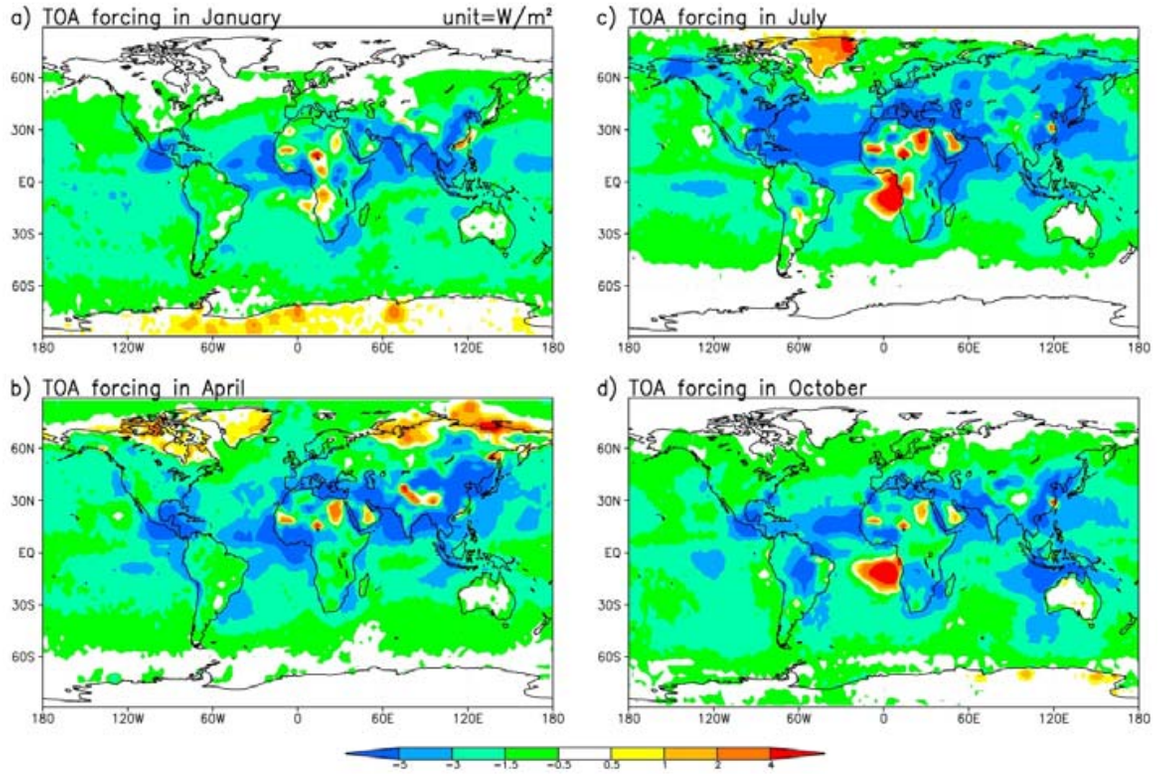

Figure 9. 2001–2009 aerosol forcing (natural + anthropogenic) estimate at the TOA. Cloud effects are included here.

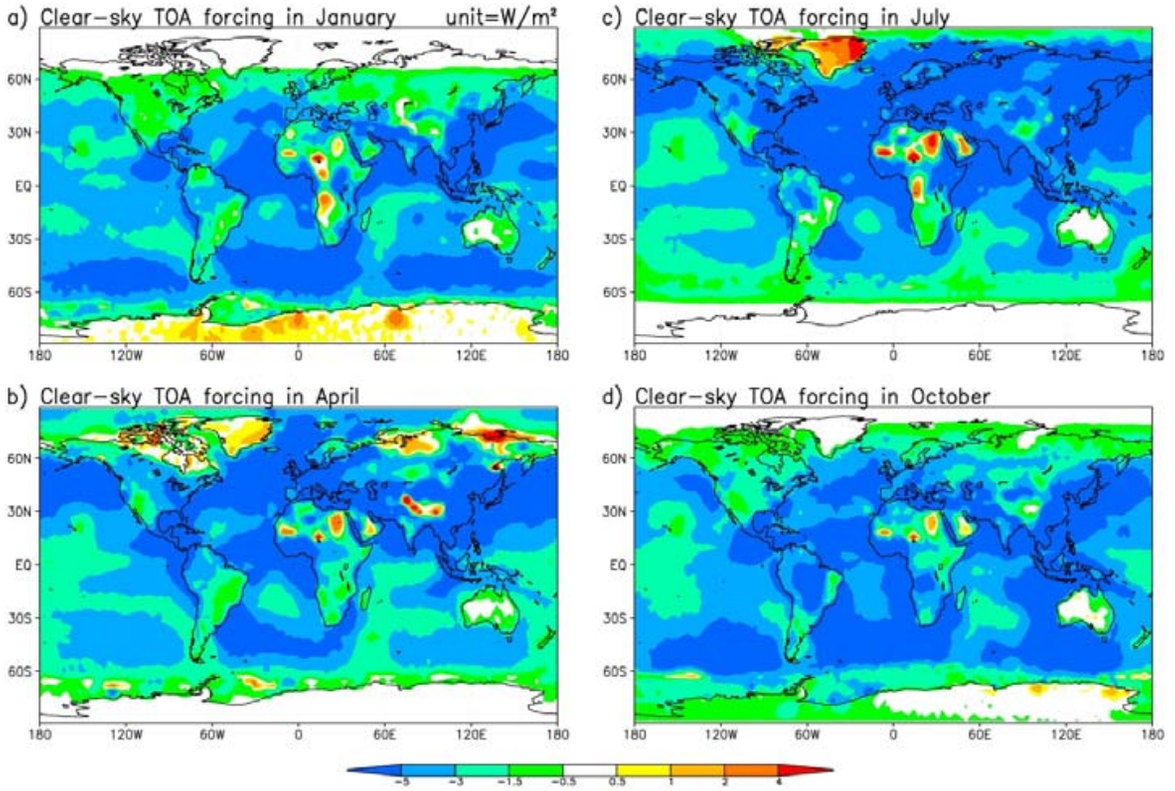

Figure 10. 2001–2009 aerosol forcing (natural + anthropogenic) estimate at the TOA. Cloud effects are not included here.

Global average aerosol forcing is summarized in Table 2. As clear in Table 2, cloud increases aerosol forcing significantly from −4.3 Wm^{-2} to −2.0 Wm^{-2}. Surprisingly, cloud decreases the atmosphere forcing slightly, indicating that the forcing enhancement by low cloud is not as much as the forcing reduction by mid or high cloud. However, this result (i.e., cloud effects on the atmosphere forcing) is sensitive to the aerosol vertical profile, and currently there is a lot of uncertainty in aerosol vertical profile. Chung et al. (2005) used an idealized profile.

	All sky	Clear sky
TOA forcing	−2.0 Wm^{-2}	−4.3 Wm^{-2}
Atmosphere forcing	+4.7 Wm^{-2}	+5.5 Wm^{-2}
Surface forcing	−6.8 Wm^{-2}	−9.7 Wm^{-2}

Table 2. Global average total (natural + anthropogenic) aerosol forcing estimates.

6. Conclusion

Thus far, I have discussed fundamental aerosol optical properties and their influences on aerosol forcing, and given an observation-constrained estimate of global aerosol forcing. Although some important topics are not discussed here, the presented material here is a good starting point in studying the science of aerosol radiative forcing in my opinion.

Author details

Chul Eddy Chung
Gwangju Institute of Science and Technology, Republic of Korea

Acknowledgement

The author would like to thank Kyunghwa Lee for her technical support. This work was supported by National Research Foundation of Korea (NRF 2012-0004055).

7. References

Alexander, D. T. L., Crozier, P. A., & Anderson, J. R., (2008), Brown carbon spheres in East Asian outflow and their optical properties, *Science*, Vol. 321, No.5890, pp. 833-836.

Andreae, M. O., & Gelencsér, A., (2006), Black carbon or brown carbon? The nature of light-absorbing carbonaceous aerosols, *Atmospheric Chemistry and Physics*, Vol. 6, No. 10, pp. 3131-3148

Chakrabarty, R. K., Moosmüller, H., Chen, L. W. A., Lewis, K., Arnott, W. P., Mazzoleni, C., Dubey, M. K., Wold, C. E., Hao, W. M., & Kreidenweis, S. M., (2010), Brown carbon in tar balls from smoldering biomass combustion, *Atmospheric Chemistry and Physics*, Vol. *10*, No. 13, pp. 6363-6370

Chung, C. E., Ramanathan, V., Kim, D., & Podgorny, I. A., (2005), Global anthropogenic aerosol direct forcing derived from satellite and ground-based observations, *Journal of Geophysical Research*, Vol. 110, No. D24, pp. D24207

Cressman, G. P., (1959), An operational objective analysis system, *Monthly Weather Review*, Vol. 87, No. 10, pp. 367-374.

Hess, M., Koepke, P., & I. Schult, (1998), Optical Properties of Aerosols and Clouds: The Software Package OPAC, *Bulletin of the American Meteorological Society*, Vol. 79, No. 5, pp. 831-844.

Hoffer, A., Gelencsér, A., Guyon, P., Kiss, G., Schmid, O., Frank, G. P., Artaxo, P., & Andreae, M. O., (2006), Optical properties of humic-like substances (HULIS) in biomass-burning aerosols, *Atmospheric Chemistry and Physics*, Vol. 6, No. 11, pp. 3563-3570.

Holben, B. N., Tanré, D., Smirnov, A., Eck, T. F., Slutsker, I., Abuhassan, N., Newcomb, W. W., Schafer, J. S., Chatenet, B., Lavenu, F., Kaufman, Y. J., Castle, J. V., Setzer, A., Markham, B., Clark, D., Frouin, R., Halthore, R., Karneli, A., O'Neill, N. T., Pietras, C., Pinker, R. T., Voss, K., & Zibordi, G., (2001), An emerging ground-based aerosol climatology: Aerosol optical depth from AERONET, *Journal of Geophysical Research*, Vol. 106, No. D11, pp. 12067-12097.

Magi, B. I., (2009), Chemical apportionment of southern African aerosol mass and optical depth, *Atmospheric Chemistry and Physics*, Vol. 9, No. 19, pp. 7643-7655.

Magi, B. I., (2011), Corrigendum to "Chemical apportionment of southern African aerosol mass and optical depth", *Atmospheric Chemistry and Physics*, Vol. 11, No.10, pp. 4777-4778.

Myhre, G., Bellouin, N., Berglen, T. F., Berntsen, T. K., Boucher, O., Grini, A. L. F., Isaksen, I. S. A., Johnsrud, M., Mishchenko, M. I., Stordal, F., & Tanré, D., (2007), Comparison of the radiative properties and direct radiative effect of aerosols from a global aerosol model and remote sensing data over ocean, *Tellus Series B: Chemical and Physical Meteorology*, Vol. 59, No. 1, pp. 115-129.

Podgorny, I. A., & Ramanathan, V., (2001), A modeling study of the direct effect of aerosols over the tropical Indian Ocean, *Journal of Geophysical Research*, Vol. 106, No. D20, pp. 24097-24105.

Stier, P., Seinfeld, J. H., Kinne, S., & Boucher, O., (2007), Aerosol absorption and radiative forcing, *Atmospheric Chemistry and Physics*, Vol. 7, No. 19, pp. 5237-5261.

Zarzycki, C. M., & Bond, T. C., (2010), How much can the vertical distribution of black carbon affect its global direct radiative forcing?, *Geophysical Research Letters*, Vol. 37, No. 20, pp. L20807.